

Effects of Antidiuretic Hormone on Urinary Acidification and on Tubular Handling of Bicarbonate in the Rat

Maurice Bichara, Odile Mercier, Pascal Houillier, Michel Paillard, and Françoise Leviel

With the technical assistance of Eric Marty

Laboratoire de Physiologie et Physiopathologie Rénale et Electrolytique, Université Paris VII, Hôpital Louis Mourier, 92701 Colombes, France; and Institut National de la Santé et de la Recherche Médicale, Paris, 75654 France

Abstract

Paired micropuncture experiments were carried out in plasma-replete volume-expanded rats to examine the acute effects of 1-desamino-8-D-arginine vasopressin (dDAVP) on urinary acidification and tubular handling of bicarbonate and chloride. No effect was detected on the fractional absorption of water, total CO₂, and chloride at end-proximal and early distal sites of superficial nephrons in intact animals; dDAVP, however, inhibited the fractional absorption of total CO₂ in Henle's loop while stimulating that of chloride in thyroparathyroidectomized (TPTX) somatostatin-infused rats. In the distal tubule accessible to micropuncture, net total CO₂ secretion was observed during hypotonic volume expansion, which reversed to net total CO₂ absorption during dDAVP infusion in intact Wistar rats. Marked stimulation of urinary acidification occurred in all animals as attested by a fall in urine pH and bicarbonate excretion. Net acid excretion almost doubled in intact rats.

We conclude that (a) antidiuretic hormone (ADH) inhibits fractional bicarbonate absorption in the thick ascending limb while stimulating that of chloride at least in TPTX somatostatin-infused rats, and (b) ADH stimulates proton secretion (or inhibits bicarbonate secretion) in the distal tubule and cortical collecting ducts, which leads to enhanced urinary acidification.

Introduction

The acute effects of antidiuretic hormone (ADH)¹ on urinary and tubular fluid acidification *in vivo* have not been directly investigated so far, to our knowledge. Yet, it has long been known that an acute water load in humans is associated with inhibition of urinary acidification and decrease in net acid excretion secondary to a fall in titratable acid excretion (1). In the latter study, evidence was presented that this was not due to the physico-chemical changes that accompany dilution of

urinary buffers; however, a direct effect of the suppression of ADH secretion attendant to the water load was not invoked to explain the inhibition of urinary acidification. Conversely, prolonged ADH administration inducing chronic hypotonic expansion in dogs with HCl-induced metabolic acidosis is associated with stimulation of urinary acidification and enhancement of net acid excretion that restore the plasma bicarbonate concentration to normal (2); in fact, in both patients with the syndrome of inappropriate secretion of antidiuretic hormone and in normal dogs subjected to chronic ADH administration, the plasma bicarbonate concentration remains within or slightly below the normal range (2, 3). Direct effects of ADH on urinary acidification were not invoked by the authors of the latter studies; rather, emphasis was laid on the role of the response of the adrenal gland to the chronic hyponatremia to explain the correction of metabolic acidosis in acidotic dogs that were administered ADH (4).

However, we have recently observed that the acute nasal insufflation of 1-desamino-8-D-arginine vasopressin (dDAVP) in a patient with pseudohypoaldosteronism type II stimulated urinary acidification as attested by a decrease in urinary pH and an increase in net acid excretion (5); acute dDAVP administration elicited a similar renal response in normal volunteers investigated in our laboratory (unpublished observations). Also, Tomita et al. (6) reported that arginine vasopressin inhibits bicarbonate secretion and/or stimulates proton secretion in cortical collecting ducts harvested from deoxycorticosterone-treated rats. These striking observations prompted us to perform the present free-flow micropuncture work, which was designed to study the effects of a dDAVP infusion in rats previously subjected to an acute hypotonic volume expansion. The results demonstrate for the first time that dDAVP greatly stimulates *in vivo* urinary acidification by increasing hydrogen secretion (or inhibiting bicarbonate secretion, or both) in the distal tubule accessible to micropuncture and, probably, in the cortical collecting tubule independent of changes in the extracellular fluid volume and plasma sodium concentration. It is also shown for the first time that dDAVP inhibits the fractional bicarbonate absorption by the superficial loop of Henle² in thyroparathyroidectomized (TPTX) somatostatin-infused rats.

Methods

Animals

12 male Sprague-Dawley rats weighing 314±10 g (mean±SE) were studied. Food was withheld 14–16 h before the experiment, but all

Address correspondence and reprint requests to Dr. M. Paillard, Laboratoire de Physiologie, Hôpital Louis Mourier, 178 Rue des Renouillers, 92701 Colombes, France.

Received for publication 17 October 1986 and in revised form 15 April 1987.

1. Abbreviations used in this paper: ADH, antidiuretic hormone; Bo, initial blood sample of 200 µl; dDAVP, 1-desamino-8-D-arginine vasopressin; GFR, glomerular filtration rate; SNGFR, single nephron glomerular filtration rate; tCO₂, total CO₂; TPTX, thyroparathyroidectomized.

J. Clin. Invest.

© The American Society for Clinical Investigation, Inc.

0021-9738/87/09/0621/10 \$2.00

Volume 80, September 1987, 621–630

2. The loop segment as used here refers to the superficial nephron segment comprised between the latest surface convolution of the proximal tubule and the earliest surface convolution of the distal tubule accessible to micropuncture.

animals had free access to water before anesthetization with Inactin (5-sec-butyl-5 ethyl-2-thiobarbituric acid, 100 mg/kg body wt). The rats were studied twice: initially for a 60-min control period during which the animals were subjected to hypotonic volume expansion to restrain the endogenous ADH secretion, and then after dDAVP (Ferring AB, Malmö, Sweden) was infused at 0.2 pg/min per g body wt during 30 min before the beginning of the second 60-min experimental period. This rate of dDAVP infusion may be assumed to induce plasma dDAVP concentrations similar to that of plasma endogenous ADH observed during antidiuresis (7).

GROUP I

Intact rats. This group was comprised of five rats in which the kidney was micropunctured twice: first, after a 7% body-wt infusion of a 75-mM NaCl solution for 60 min followed by a sustaining infusion at 0.3 μ l/min per g body wt during 2 h of equilibration; the latter protocol is similar to that described previously by other investigators (8), which is shown to inhibit the endogenous ADH secretion; and second, after 30 min of dDAVP infusion while the 75-mM NaCl infusion rate was diminished so that the total rate of the infused solutions only balanced the reduced urinary flow rate. During the two periods, each tubule was punctured twice: at early distal and then at end proximal sites.

GROUP II

TPTX rats infused with somatostatin. This group was comprised of seven rats that were studied exactly as the animals of group I except that they were acutely TPTX and infused with somatostatin (0.7 ng/min per g body wt) early during the preparatory surgery. The protocol in this group was designed to study the renal and nephron effects of dDAVP (a) in the absence of other polypeptide hormones (parathyroid hormone, calcitonin, and glucagon) that were shown to activate the adenylate cyclase in the same nephron segments as ADH (9) and thus that could mask possible tubular effects of ADH when they are present, and (b) in the absence of possible variations in parathyroid hormone and glucagon activities and of phosphate in the urine since we showed that these factors are important determinants of urine and tubule fluid acidification (10–12).

GROUP III

Intact Wistar rats. Six more rats weighing 286 ± 7 g made up this group in which each tubule was punctured at late and then at early distal sites. We used Wistar rats to study the distal tubule because it is well established that in this strain the initial cortical collecting tubule represents 45% of the total length of the subcapsular distal tubule accessible to micropuncture (13); thus, in this particular strain of rats, both the distal convoluted tubule (early distal) and the initial cortical collecting tubule (late distal) are accessible to micropuncture (13). Note that the intercalated cells that are involved in H^+ and bicarbonate transports are present in both segments in addition to the distal convoluted tubule cells, the connecting tubule cells, and the principal cells of the initial cortical collecting tubule (14). We did not determine the precise sites of micropuncture; the longest distal tubules were selected, judging by the presence of an apparently long segment between the first and the last accessible loop. The fact that the initial cortical collecting tubule was really included in the distal segments studied so far is fully established by noting that significant water absorption occurred in all the tubules punctured during dDAVP infusion and at a lesser degree during hypotonic expansion, as will be shown in Results.

Micropuncture protocol

The animals were surgically prepared for micropuncture as previously described (10, 15–17). After anesthetization, the rats were placed on a servo-regulated heated micropuncture table that maintained their rectal temperature at 37°C. A catheter (PE-50; Biotrol, Paris, France) was inserted into the left femoral artery for continuous monitoring of blood pressure and for blood sampling. Immediately after arterial catheterization, a blood sample of 210 μ l, hereafter referred to as the Bo sample, was obtained for determination of the initial hematocrit and plasma sodium concentration. This and all subsequent blood samples

were quantitatively replaced by whole blood obtained on the morning of study from another rat that was intact for groups I and III and was TPTX the day before for group II. A tracheostomy was performed and PE-50 catheters were inserted into both external jugular veins for infusions. In the rats of group II, the thyroparathyroidectomy was made just before the tracheostomy. A 0.05- μ l/min per g body-wt infusion of a Ringer solution was begun; the Ringer solution contained 85 mM NaCl, 25 mM KCl, 25 mM $NaHCO_3$, 3.6 mM $CaCl_2$, 4 mM Na_2HPO_4 , 2 mM $MgSO_4$, and 5 mM glucose. There was no Na_2HPO_4 in the Ringer solution infused in the TPTX rats of group II to minimize the rise in the plasma phosphate concentration that is produced by the thyroparathyroidectomy. Somatostatin (Clin-Midy Laboratoire, Paris, France) was added to the Ringer solution in group II to achieve a 0.7-ng/min per g body-wt infusion rate, which was shown to inhibit the endogenous glucagon secretion (18). The left kidney was then exposed and stabilized through an abdominal approach and bathed continuously with a paraffin oil drip. The oil was equilibrated with a 100-mM HEPES–25-mM $NaHCO_3$ solution and bubbled with 5% CO_2 . The left ureter and the bladder were cannulated with PE-50 tubing. An amount of 1.3% body wt of plasma obtained from another rat that was intact in groups I and III and was TPTX the day before in group II was infused to compensate for the loss of plasma caused by the preparatory surgery (plasma repletion). In group III, but not in groups I and II that were first studied, the plasma repletion was followed by a maintenance infusion of plasma at 0.03 μ l/min per g body wt through a femoral vein, as previously described (15). As will be shown in Results, the maintenance infusion of plasma resulted in a more efficient plasma repletion (as judged by the hematocrit values) in group III than in groups I and II; in these latter two groups, the hematocrits and plasma protein concentrations were nevertheless stable throughout the experiments. After plasma repletion, the Ringer solution infusion was continued through one jugular catheter at 0.05 μ l/min per g body wt. Hypotonic volume expansion was performed through the other jugular catheter: an amount equal to 7% body wt of a 75-mM NaCl solution was infused in 60 min, followed by a sustaining infusion at 0.3 μ l/min per g body wt. A priming dose of 80 μ Ci of [methoxy- 3H]inulin (New England Nuclear, Boston, MA) was given, followed by a sustaining infusion of 200 μ Ci/h in the Ringer solution.

After an equilibration period of 2 h, a first 60-min period of micropuncture (hypotonic expansion) was begun. Each tubule was punctured at early distal and then at end proximal sites in groups I and II, and at late and then at early distal sites in group III. The various micropuncture sites were identified and mapped during the equilibration period by injecting 1 or 2 nl of a 1% lissamine green solution in a proximal loop by a sharpened glass pipette with an outside tip diameter of 4 μ m. Exactly timed 3–8-min collections for determination of flow rates and of inulin, chloride, and total CO_2 (tCO_2) concentrations were performed using sharpened glass pipettes with outside tip diameters of 6–8 μ m. The tubules were blocked by an injection of paraffin oil stained with Sudan black B and equilibrated with a 100-mM HEPES–25-mM $NaHCO_3$ solution and bubbled with 5% CO_2 .

After the first period of micropuncture, dDAVP was added to the Ringer solution to achieve a 0.2 pg/min per g body wt dDAVP infusion rate. The Ringer solution infusion rate was the same as during the control period (i.e., 0.05 μ l/min per g body wt), but the 75-mM NaCl solution infusion rate was reduced to avoid an increase in the volume expansion since dDAVP greatly decreased the urinary flow rate. For the 18 rats studied, the total infusion rate was 1.1 ± 0.1 ml/h whereas the total urinary flow rate, 0.9 ± 0.1 ml/h (mean \pm SE; NS). After a 30-min equilibration period, the second 60-min period of micropuncture (dDAVP) was begun, during which fresh tubules were punctured.

During each of the two micropuncture periods, one or two timed urine collections were made for determination of urine flow rate, whole-kidney glomerular filtration rate (GFR), and sodium, potassium, chloride, inorganic phosphorus, calcium, magnesium, and tCO_2 excretory rates. Also, urinary osmolality, urinary pH and PCO_2 , and titratable acid and ammonium contents were determined in the fresh urine samples. The urinary bicarbonate concentration was calculated

as the difference between the measured $t\text{CO}_2$ and dissolved CO_2 ($0.031 \times \text{PCO}_2$). The urine was collected under water-equilibrated paraffin oil. Blood samples of 600 μl each were obtained at the beginning and end of the two micropuncture periods for determination of hematocrit, and protein, sodium, potassium, chloride, inorganic phosphorus, calcium, magnesium, and [methoxy- ^3H]inulin plasma concentrations. Arterial pH and PCO_2 , and plasma $t\text{CO}_2$ concentration were also determined in each blood sample.

After the completion of the experiment, the left kidney was excised, blotted, and weighed.

Analytical procedures

Analytical procedures were performed as previously described (10, 15, 17). Briefly, $t\text{CO}_2$ (dissolved CO_2 and HCO_3^-) and chloride were measured in the tubule fluid samples by microcalorimetry (19) and the electrometric titration method of Ramsay et al. (20), respectively. The [methoxy- ^3H]inulin radioactivity in plasma, urine, and tubule fluid was measured by scintillation counting (Betamatic; Kontron, Traffes, France). Urinary titratable acid and ammonium contents were determined by automated titration methods. Net acid excretion rate was calculated as the sum of that of urinary ammonium and titratable acid minus bicarbonate. Other standard analytical procedures have been previously described in detail (15, 17).

Calculations

The calculations were made exactly as previously described (15). The single nephron glomerular filtration rate (SNGFR) calculated from the early distal flow rate and inulin concentration was used in calculations for estimating the handling of water, $t\text{CO}_2$, and chloride by the loop of Henle in groups I and II; in group III, the mean of the SNGFR values obtained from late and early distal sites was used in calculations; mean late distal and early distal SNGFR values were 29.5 ± 2.0 and 30.1 ± 1.9 nl/min (NS; $n = 14$), respectively. The ultrafiltrate concentrations of calcium, inorganic phosphorus, and magnesium were taken as 0.60, 0.93, and 0.80 times plasma water concentrations (21), respectively.

The results obtained from left and right kidneys were similar; thus, only those from the left-micropunctured kidney are presented. All absolute rates were factored by kidney weight to compensate for differences caused by animal size. Kidney weights ranged from 0.91 to

1.39 g with a mean value of 1.23 ± 0.04 g for Sprague-Dawley rats, and from 0.87 to 1.10 g with a mean value of 0.99 ± 0.01 g for Wistar rats.

Results are expressed as means \pm SE. Statistical significance was assessed by the two-tailed, paired or unpaired t test, as appropriate.

Results

Blood composition. Mean arterial pressure did not vary during dDAVP infusion in the three groups (105 ± 5 vs. 100 ± 5 mmHg in group I, 109 ± 4 vs. 102 ± 3 mmHg in group II, and 102 ± 5 vs. 101 ± 5 mmHg in group III). Hematocrits and plasma protein concentrations remained unchanged, which reflects maintenance of the plasma volume and probably of the extracellular fluid volume of the animals (Table I). Note that the initial hematocrit in the Bo sample was slightly, although not significantly, lower than the hematocrit during the experimental periods in the intact rats of group I; thus, the intact rats of group III were subjected to a maintenance infusion of plasma, and, judging by the hematocrit values, these latter rats may have been more effectively plasma replete. In the TPTX somatostatin-infused rats of group II, the hematocrit values during the experimental periods were not significantly different from that in the initial Bo sample. Whereas the initial Bo plasma sodium concentration was 154 ± 3 mM in groups I and II, it decreased to 151 ± 1 mM in group I and to 148 ± 3 mM in group II ($P < 0.01$ for each) as a result of the hypotonic volume expansion; also, in group III of Wistar rats, the plasma sodium concentration decreased from 149 ± 3 mM in the Bo sample to 146 ± 3 mM ($P < 0.05$) after hypotonic expansion; the plasma sodium concentration then remained stable during the hypotonic expansion and dDAVP periods in the three groups. The arterial pH slightly increased in all groups; the plasma calcium concentration continued to decrease in the TPTX rats of group II during dDAVP infusion. The changes in arterial pH and in the plasma calcium concentration were, however, very

Table I. Arterial Blood Composition

Period	Hematocrit	Protein	Na	K	Cl	Ca	Pi	Mg	$t\text{CO}_2$	pH	PCO_2
	vol %	g/dl	mM	mM	meq/liter	mM	mM	mM	mM		mmHg
Group I*											
Hypotonic expansion	48.9 ± 1.0	4.2 ± 0.2	151 ± 1	4.4 ± 0.2	110 ± 1	2.09 ± 0.05	2.05 ± 0.04	0.68 ± 0.03	25.7 ± 1.0	7.44 ± 0.01	36 ± 2
dDAVP	49.8 ± 1.3	4.2 ± 0.2	151 ± 2	4.4 ± 0.3	109 ± 1	2.12 ± 0.11	2.12 ± 0.07	0.69 ± 0.06	26.4 ± 2.1	7.47 ± 0.01	35 ± 1
P	NS	NS	NS	NS	NS	NS	NS	NS	NS	<0.01	NS
Group II†											
Hypotonic expansion	47.7 ± 0.8	4.2 ± 0.1	148 ± 3	4.1 ± 0.3	107 ± 1	1.51 ± 0.05	3.2 ± 0.3	0.53 ± 0.02	25.5 ± 0.3	7.43 ± 0.01	37 ± 1
dDAVP	49.6 ± 0.9	4.2 ± 0.1	148 ± 2	4.0 ± 0.2	106 ± 1	1.33 ± 0.03	3.1 ± 0.1	0.51 ± 0.01	26.1 ± 0.3	7.46 ± 0.01	36 ± 1
P	NS	NS	NS	NS	NS	<0.05	NS	NS	NS	<0.05	NS
Group III‡											
Hypotonic expansion	45.4 ± 1.1	3.9 ± 0.2	146 ± 3	3.8 ± 0.1	113 ± 1	ND	2.29 ± 0.10	ND	22.4 ± 0.8	7.40 ± 0.01	35 ± 2
dDAVP	45.8 ± 1.2	3.8 ± 0.2	145 ± 2	3.6 ± 0.1	111 ± 1	ND	2.32 ± 0.10	ND	23.0 ± 0.7	7.44 ± 0.01	32.5 ± 1.5
P	NS	NS	NS	NS	NS		NS		NS	<0.01	<0.01

Values are means \pm SE. Pi, inorganic phosphorus. Vol %, percentage of total volume of blood. * Five intact rats (Bo-hematocrit, 46.9 ± 1.1 vol%). † Seven TPTX somatostatin-infused rats (Bo-hematocrit, 47.2 ± 0.7 vol%). ‡ Six intact Wistar rats (Bo-hematocrit, 44.8 ± 0.7 vol%).

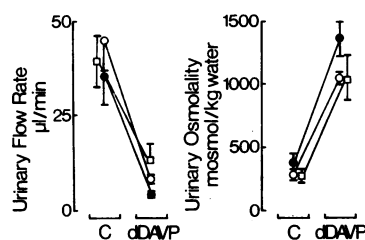


Figure 1. Mean values \pm SE of urinary flow rates and osmolalities in five intact Sprague-Dawley rats (\circ), seven TPTX somatostatin-infused rats (\bullet), and six intact Wistar rats (\square). C, hypotonic expansion control period; dDAVP, dDAVP period. All variations are significant at the $P < 0.02$ level.

slight and could not explain the stimulation of urinary acidification described below.

Whole-kidney GFR and urinary excretion rates. As shown in Fig. 1, dDAVP infusion decreased the urinary flow rate and increased the urinary osmolality in all groups. Note that the mean values of urinary osmolality, i.e., 284 ± 34 , 385 ± 75 , and 279 ± 18 mosmol/kg H_2O in groups I, II, and III, respectively, were not maximally low during the first period, which indicates that the endogenous ADH secretion was not completely suppressed; nevertheless, the urinary osmolality was readily below 300 mosmol/kg H_2O in several rats, which clearly demonstrates that the endogenous ADH secretion was effectively restrained by the hypotonic expansion. The whole-kidney GFR significantly decreased in all groups during dDAVP infusion (Table II). The effects of dDAVP on the electrolyte excretion rates differed, however, in the intact and TPTX somatostatin-infused rats. The urinary excretion rates of sodium, potassium, chloride, calcium, and magnesium were not affected by dDAVP in the intact rats of groups I and III; the urinary phosphate excretion rate significantly decreased in groups I and III as a result of the reduction in the phosphate-filtered load; the urinary phosphate fractional excretion did not significantly vary from 0.27 ± 0.03 to 0.22 ± 0.02 in group I, and from 0.20 ± 0.02 to 0.16 ± 0.02 in group III. However, be-

cause of the reduction in the urinary flow rate, the urinary phosphate concentration increased from 15 ± 3 to 57 ± 8 mM ($P < 0.001$) in group I, and from 15 ± 3 to 35 ± 8 mM ($P < 0.05$) in group III. In contrast, the urinary excretion rates of sodium, potassium, chloride, calcium, and magnesium sharply decreased during dDAVP infusion in the TPTX somatostatin-infused rats of group II. In particular, the fractional excretion of calcium and magnesium decreased from 0.031 ± 0.008 to 0.003 ± 0.001 ($P < 0.02$) and from 0.11 ± 0.01 to 0.04 ± 0.01 ($P < 0.001$), respectively. In this latter group, the urinary phosphate excretion rate was very low during the two periods; the urinary phosphate concentration did not significantly vary from 0.9 ± 0.3 to 2.4 ± 0.7 mM (NS).

As shown in Fig. 2, dDAVP infusion dramatically stimulated urinary acidification in groups I and II. The urinary pH decreased from 6.74 ± 0.07 to 5.45 ± 0.07 ($P < 0.001$) in group I and from 6.90 ± 0.11 to 5.92 ± 0.09 ($P < 0.01$) in group II. There was no more bicarbonate in the urine in both groups during dDAVP infusion. Titratable acid excretion increased from 204 ± 64 to 428 ± 76 nmol/min ($P < 0.05$) in the intact rats of group I; titratable acid excretion also increased from 22 ± 7 to 41 ± 7 nmol/min ($P < 0.05$), but was very low in the TPTX somatostatin-infused rats of group II. The urinary ammonium excretion rate did not significantly vary in both groups. As a result of these effects, the urinary net acid excretion significantly increased from 668 ± 131 to $1,142 \pm 84$ nmol/min ($P < 0.05$) in group I, but not in group II in which there was minimal amount of titratable acid in the urine.

In group III, we only measured the urinary pH and bicarbonate excretion rate that significantly decreased from 6.13 ± 0.11 to 5.34 ± 0.03 nmol/min and from 45 ± 24 to 1 ± 0.5 nmol/min, respectively, as in the other groups.

Effects of dDAVP on the loop handling of water, tCO_2 , and chloride. The results of the micropuncture data are summarized in Tables III and IV. The SNGFR significantly decreased, as did the whole-kidney GFR, in both groups. In the intact rats of group I, the dDAVP infusion had no detectable

Table II. Whole-Kidney GFR and Urinary Excretion Rates

Period	GFR	Urinary excretion rate					
		Na	K	Cl	Pi	Ca	Mg
	ml/min	nmol/min	nmol/min	neq/min	nmol/min	nmol/min	nmol/min
Group I*							
Hypotonic expansion	1.07 ± 0.04	$2,210 \pm 753$	898 ± 247	$3,008 \pm 502$	569 ± 44	7 ± 3	49 ± 14
dDAVP	0.86 ± 0.04	$1,365 \pm 192$	949 ± 111	$2,605 \pm 299$	401 ± 38	6 ± 2	47 ± 10
P	< 0.05	NS	NS	NS	< 0.05	NS	NS
Group II†							
Hypotonic expansion	1.07 ± 0.07	$1,598 \pm 453$	$1,228 \pm 154$	$2,896 \pm 536$	19 ± 4	31 ± 9	52 ± 5
dDAVP	0.82 ± 0.03	380 ± 118	676 ± 100	$1,657 \pm 244$	10 ± 2	2 ± 0.5	12 ± 2
P	< 0.01	< 0.02	< 0.05	< 0.05	NS	< 0.02	< 0.02
Group III‡							
Hypotonic expansion	1.19 ± 0.03	$2,372 \pm 506$	$1,063 \pm 96$	$3,086 \pm 504$	542 ± 54	ND	ND
dDAVP	0.98 ± 0.02	$2,462 \pm 762$	$1,203 \pm 123$	$3,685 \pm 813$	346 ± 38	ND	ND
P	< 0.01	NS	NS	NS	< 0.05		

Values are means \pm SE. All rates were factored by kidney weight. Pi, inorganic phosphorus. * Five intact rats. † Seven TPTX somatostatin-infused rats. ‡ Six intact Wistar rats.

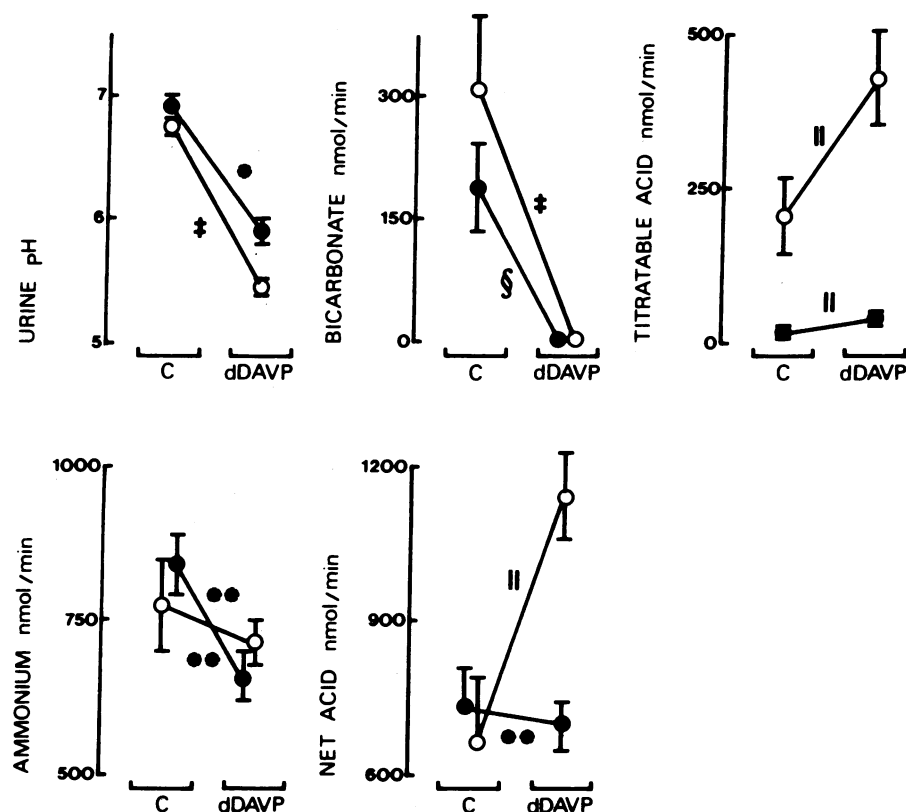


Figure 2. Mean values \pm SE of urine pH and urinary excretion rates, factored by kidney weight, of bicarbonate, titratable acid, ammonium, and net acid in five intact rats (\circ) and seven TPTX somatostatin-infused rats (\bullet). C, hypotonic expansion control period; dDAVP, dDVAP period. *, $P < 0.001$; †, $P < 0.01$; §, $P < 0.02$; ||, $P < 0.05$; **, NS.

tubular effects on the fractional absorption of water, tCO_2 , and chloride until the early distal site; in particular, dDAVP did not modify the fractional absorption of tCO_2 and chloride in Henle's loop. In contrast, dDAVP increased the capability of the loop to absorb chloride and decreased that for tCO_2 in the TPTX somatostatin-infused rats of group II. This is attested by a significant increase in the loop chloride fractional absorption and by a significant decrease in the loop tCO_2 fractional ab-

sorption during dDAVP infusion, whereas the loads delivered to the loop did not vary significantly (Table IV). It should also be pointed out that the early distal chloride concentration significantly decreased whereas that of tCO_2 significantly increased in the presence of dDAVP in group II (Table III); as a result, the tubular fluid-to-ultrafiltrate concentration ratio at the early distal site decreased for chloride (from 0.39 ± 0.01 to 0.32 ± 0.01 ; $P < 0.01$) and increased for tCO_2 (from 0.18 ± 0.01

Table III. Micropuncture Data in Sprague-Dawley Rats

Period	Early distal SNGFR	Tubular fluid flow rate		TF/P Inulin		tCO_2 concentration		Chloride concentration	
		End proximal	Early distal	End proximal	Early distal	End proximal	Early distal	End proximal	Early distal
	nl/min	nl/min	nl/min			mM	mM	meq/liter	meq/liter
Group I*									
Hypotonic expansion (15 tubules)	36.1 ± 2.1	21.5 ± 0.9	12.3 ± 0.8	1.67 ± 0.04	3.00 ± 0.14	8.0 ± 0.9	4.6 ± 0.5	140 ± 1	44 ± 2
dDAVP (18 tubules)	28.1 ± 2.1	16.9 ± 1.1	8.7 ± 0.6	1.65 ± 0.06	3.27 ± 0.17	9.3 ± 1.0	6.4 ± 0.8	138 ± 2	47 ± 1
P	<0.001	<0.001	<0.001	NS	NS	NS	NS	NS	NS
Group II†									
Hypotonic expansion (21 tubules)	33.3 ± 1.6	16.7 ± 1.2	8.4 ± 0.6	2.08 ± 0.09	4.20 ± 0.25	7.3 ± 0.6	5.2 ± 0.4	141 ± 1	46 ± 2
dDAVP (23 tubules)	26.1 ± 1.3	13.7 ± 0.9	7.0 ± 0.5	1.98 ± 0.08	3.99 ± 0.22	9.1 ± 0.9	7.1 ± 0.7	138 ± 2	38 ± 1
P	<0.001	NS	NS	NS	NS	NS	<0.05	NS	<0.05

Values are means \pm SE. Absolute rates were factored by kidney weight. TF/P, tubular fluid-to-plasma concentration ratio. * Five intact rats. † Seven TPTX somatostatin-infused rats.

Table IV. Henle's Loop Handling of tCO₂ and Chloride

Period	tCO ₂			Chloride		
	End proximal delivery	Henle's loop absolute absorption	Henle's loop fractional absorption	End proximal delivery	Henle's loop absolute absorption	Henle's loop fractional absorption
	pmol/min	pmol/min		peq/min	peq/min	
Group I*						
Hypotonic expansion (15 tubules)	172±22	113±16	0.66±0.03	2,996±130	2,458±109	0.823±0.012
dDAVP (18 tubules)	157±20	103±14	0.65±0.02	2,324±158	1,915±130	0.824±0.007
<i>P</i>	NS	NS	NS	<0.001	<0.001	NS
Group II†						
Hypotonic expansion (21 tubules)	122±13	80±10	0.64±0.02	2,439±217	2,047±205	0.829±0.009
dDAVP (23 tubules)	124±13	75±9	0.58±0.02	1,957±140	1,674±120	0.857±0.006
<i>P</i>	NS	NS	<0.05	NS	NS	<0.02

Values are means±SE. Absolute rates were factored by kidney weight. * Five intact rats. † Seven TPTX somatostatin-infused rats.

to 0.25±0.02; *P* < 0.05) in the presence of dDAVP. In other words, the capability of the thick ascending limb to establish a transepithelial concentration gradient was increased for chloride and decreased for tCO₂ by dDAVP in TPTX somatostatin-infused rats. Note, however, that in our experimental conditions the absolute absorption rates of chloride and tCO₂ in the loop were not significantly different before and after dDAVP (Table IV), probably because of tubular heterogeneity and scatter of the data (recollections were impossible in this micropuncture protocol). Also, the early distal delivery of tCO₂ did not significantly vary either in group I (from 59±9 to 54±7 pmol/min; NS) or in group II (from 42±4 to 50±5 pmol/min; NS). Thus, the stimulation of urinary acidification observed in both groups during dDAVP infusion may have been explained by effects in more distal parts of the nephron, i.e., in the distal tubule and/or collecting ducts.

Effects of dDAVP in the distal tubule accessible to micropuncture in Wistar rats (group III). The data are summarized in Table V and Figs. 3 and 4. As in the intact Sprague-Dawley rats of group I, the SNGFR as well as the early distal tubular fluid flow rate slightly decreased during the dDAVP infusion; the early distal chloride delivery also tended to decrease, although not significantly, but the early distal tCO₂ delivery remained strictly constant from 41±6 to 47±7 pmol/min. As

shown in Figs. 3 and 4, the very striking observation in the distal tubule was that net tCO₂ secretion was noted during hypotonic expansion, which reversed to net tCO₂ absorption during the dDAVP infusion. Net tCO₂ secretion occurred in all tubules, but one with a mean value of 13±6 pmol/min (significantly different from zero, *P* < 0.05) during the first period, and the tCO₂ concentration in the tubular fluid increased from 4.0±0.6 to 5.8±0.5 mM (*P* < 0.05) along the distal tubule. During the dDAVP infusion, net tCO₂ absorption was observed in all tubules with a mean value of 19±3 pmol/min, and the tCO₂ concentration tended to decrease, although not significantly, from 5.5±0.5 to 4.8±0.8 mM along the distal tubule despite water absorption. As a result, the late distal tCO₂ delivery significantly decreased from 54±8 pmol/min during hypotonic expansion to 28±7 pmol/min (*P* < 0.01) during dDAVP infusion. Thus, it is clear that dDAVP inhibited bicarbonate secretion or stimulated proton secretion (bicarbonate absorption), or both, in the distal tubule accessible to micropuncture in Wistar rats.

As shown in Fig. 3, dDAVP also enhanced water and chloride fractional absorption along the distal tubule, as expected. The tubular fluid-to-plasma inulin concentration ratio increased from early to late distal puncture sites in all the tubules studied during dDAVP infusion. These observations indicate

Table V. Effects of dDAVP in the Distal Tubule of Six Intact Wistar Rats (Group III)

Period	SNGFR	Early distal delivery			TF/P inulin		TF/UF tCO ₂		TF/UF chloride	
		H ₂ O	tCO ₂	Chloride	Early distal	Late distal	Early distal	Late distal	Early distal	Late distal
	nl/min	nl/min	pmol/min	peq/min						
Hypotonic expansion (six tubules)	32.2±2.4	10.5±1.1	41±6	393±54	3.13±0.13	3.59±0.19*	0.18±0.02	0.24±0.02*	0.30±0.02	0.22±0.02*
dDAVP (eight tubules)	28.3±2.1	8.4±0.6	47±7	343±40	3.40±0.24	5.52±0.55†	0.22±0.03	0.19±0.03	0.33±0.03	0.25±0.03*
<i>P</i>	<0.05	<0.05	NS	NS	NS	<0.05	NS	<0.05	NS	NS

Values are means±SE. Absolute rates were factored by kidney weight. TF/P and TF/UF, tubular fluid-to-plasma and -to-ultrafiltrate concentration ratio. * *P* < 0.05 and † *P* < 0.01, as compared with the early distal value.

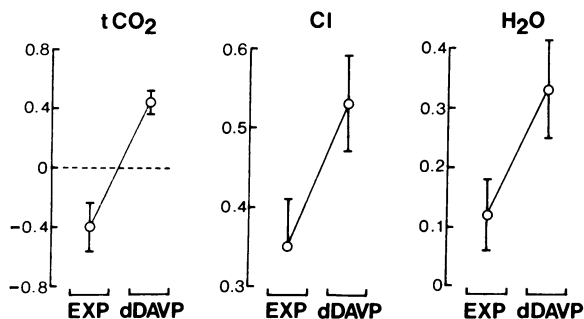


Figure 3. Mean values \pm SE of fractional absorption of tCO₂ ($P < 0.001$), chloride ($P < 0.05$), and water ($P < 0.05$) in superficial distal tubules of six Wistar rats during hypotonic expansion (EXP) and dDAVP infusion (dDAVP). Negative values denote fractional secretion.

that a significant moiety of initial cortical collecting tubule was present between the two puncture sites since it is established that ADH increases the water permeability only in the principal cells of the initial cortical collecting tubule (13). Also, note that the fractional absorption of water along the distal tubule was rather low (0.12 ± 0.06) during hypotonic expansion, which confirms that the endogenous ADH secretion was effectively restrained by the experimental protocol.

Discussion

The aim of the present study was to examine, for the first time in vivo, the acute effects of dDAVP, an arginine vasopressin analogue that is devoid of vascular action, on urinary acidification and simultaneously on the nephron segmental handling of bicarbonate and chloride in the rat. For this purpose and the following reasons, we used TPTX somatostatin-infused Sprague-Dawley rats as well as intact animals. First, when studying urinary acidification, it is necessary to control the endogenous secretion of parathyroid hormone and glucagon and the urinary phosphate concentration since we showed previously (10–12) that these factors are important determinants of urine and tubule fluid acidification. Second, since parathyroid hormone, calcitonin, and glucagon have same target cells as ADH in the renal tubule and particularly in the thick ascending limb (9), it may be easier to detect possible tubular effects of ADH

in Henle's loop in the absence rather than in the presence of these other hormones. Each rat was subjected to hypotonic volume expansion that restrained, but not completely suppressed the endogenous secretion of ADH as attested by low urinary osmolalities and high urinary flow rates during the first control periods; then, the animal was infused with dDAVP that induced physiological antidiuretic activities as attested by less than maximally high urinary osmolalities and low urinary flow rates. The dDAVP infusion greatly stimulated urinary acidification in both intact and TPTX somatostatin-infused rats. The stimulation of the proton secretion (or inhibition of bicarbonate secretion) took place in the distal tubule accessible to micropuncture and thus probably in cortical collecting tubules. Also, dDAVP inhibited the bicarbonate fractional absorption in Henle's loop as evidenced in TPTX somatostatin-infused animals. These various acute effects were directly due to the dDAVP administration since other factors known to acutely affect urinary acidification, such as the plasma acid-base status (22), the plasma calcium concentration (17), the plasma and extracellular fluid volumes (15), and parathyroid hormone and glucagon secretion (10, 12) were controlled in our study.

The whole-kidney GFR and SNGFR slightly decreased during the dDAVP infusion in all animals; this result is consistent with the fact that ADH was shown to lower the glomerular ultrafiltration coefficient in the rat (23). The fractional reabsorption of water, bicarbonate, and chloride in the proximal convoluted tubule was not affected during the dDAVP period in both intact and TPTX somatostatin-infused rats. This stability of the proximal tubule functions during the course of our experiments also confirms that the extracellular fluid volume, which we showed to modulate the proximal handling of water, bicarbonate, and chloride (15, 16), was stable. Whereas dDAVP had no detectable effects on the loop absorption of bicarbonate and chloride in intact rats, it significantly inhibited the bicarbonate fractional absorption in Henle's loop while stimulating that of chloride in TPTX somatostatin-infused rats. Although we did not detect significant differences in the absolute rates of chloride and bicarbonate absorption in the loop, our data, as discussed in Results, clearly show that the capability of the thick ascending limb to establish a transepithelial concentration gradient was increased for chloride and decreased for bicarbonate in TPTX somatostatin-infused rats. These results are in agreement with those obtained in a previous free-flow micropuncture study that showed dDAVP stimulates the loop chloride absorption in TPTX glucose-infused Brattleboro rats (7). Another recent work also demonstrated by the in vivo loop micropuncture technique that vasopressin stimulates the loop absorption of chloride in intact Brattleboro rats (24). The bicarbonate absorption in Henle's loop was not studied in these latter works (7, 24). The effects of dDAVP in Henle's loop observed in the present study could have been located in the proximal pars recta, in the thin descending limb in the inner stripe of outer medulla, or in the thick ascending limb since superficial nephrons have short loops that contain only these three segments. Several considerations, however, strongly suggest that dDAVP acted on the thick ascending limb. First, ADH was shown to stimulate the adenylate cyclase activity in the cortical and particularly medullary thick ascending limb and not in the proximal tubule or in the thin descending limb of rat kidney (9). Second, ADH enhanced chloride absorption by the me-

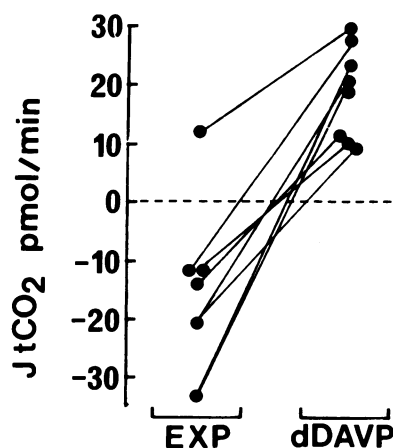


Figure 4. Absolute values of net tCO₂ flux (J_{tCO_2} ; $P < 0.001$) along the distal tubule in Wistar rats. Negative values denote net secretion; positive values, net absorption. Each point represents the value obtained in one tubule. Lines connect results obtained in the same rat. EXP, hypotonic expansion; dDAVP, dDAVP infusion.

dullary thick ascending limb perfused in vitro of mouse (25, 26) and rat (24). Third, Good and co-workers (27, 28) have demonstrated that bicarbonate is actively absorbed in the thick ascending limb of rat kidney and that inhibition of chloride absorption by furosemide is accompanied with stimulation of bicarbonate absorption in the cortical segment. Finally, it may be pointed out that the effects of dDAVP detected in the loop of TPTX somatostatin-infused rats of the present study were accompanied with significant decrease in the calcium and particularly magnesium absolute and fractional urinary excretion; the dDAVP-induced reduction in the magnesium urinary excretion has been shown to directly result from dDAVP-stimulated magnesium absorption in the thick ascending limb, but not in the distal tubule of TPTX glucose- or somatostatin-infused Brattleboro rats (7, 29). Accordingly, no effect of dDAVP was detected in the loop of intact rats of the present study in which the dDAVP infusion failed to alter the calcium and magnesium urinary excretion rates. Presumably, we did not detect dDAVP effects in the loop of intact rats because of the presence in these animals of parathyroid hormone, calcitonin, and glucagon circulating activities. The early distal bicarbonate delivery nevertheless did not significantly vary in our groups of rats. As shown by results obtained in Wistar rats in the present study, the stimulation of urinary acidification observed during the dDAVP infusion occurred in the distal tubule and thus probably in cortical collecting tubules. A contribution to the observed results of more proximal parts of the deep nephrons not accessible to micropuncture cannot be excluded but seems unlikely. First, the dDAVP-induced inhibition of bicarbonate absorption by the thick ascending limb of superficial nephrons should also have occurred in the medullary thick ascending limb of deep nephrons. Second, the process of urine concentration during antidiuresis was shown to alkalinize the tubular fluid as it flows down the thin descending limb of juxtamedullary nephrons secondary to water abstraction and CO₂ diffusion (30); also, the absence of transepithelial bicarbonate concentration gradient across the thin ascending limb makes it unlikely that passive bicarbonate absorption could occur in this latter segment (30).

The results obtained in the present study in Wistar rats demonstrate that ADH exerts a major effect on bicarbonate transport in the distal tubule. We found that net bicarbonate secretion took place in distal tubules during hypotonic volume expansion that restrained the endogenous ADH secretion, whereas net bicarbonate absorption occurred when dDAVP was administered. This striking observation is similar to that of Tomita et al. (6) whereby in the cortical collecting duct harvested from deoxycorticosterone-treated rats isolated and perfused in vitro, the addition of arginine vasopressin to the peritubular bath changed initial net bicarbonate secretion to net bicarbonate absorption. Clearly, the effect of dDAVP in the distal tubule explained, at least in part, the marked stimulation of acidification of the final urine observed in the present study since the late distal tCO₂ delivery significantly decreased by almost 50%. Thus, dDAVP inhibited bicarbonate secretion or stimulated proton secretion, or both, in the distal tubule, and it is likely that this effect also occurred in the cortical collecting tubule. The distal tubule accessible to micropuncture is a heterogeneous segment successively composed in Wistar rats of a distal convoluted tubule (48.3%), a small connecting tubule (6.7%), and an initial cortical collecting tubule

(45%) (13). Intercalated cells that are believed to be responsible for the proton and bicarbonate transports are present in these three segments, which reach 37–39% of the cells in the initial cortical collecting tubule (14). In fact, it is known that there are two types of intercalated cells, one being capable of bicarbonate secretion, and the other of proton secretion (bicarbonate absorption) (see reference 14 for review). Whereas it is established that ADH increases the water permeability of only the principal cells of the cortical collecting tubule (13), it is unknown whether it acts directly on the intercalated cells and thus on the H⁺/bicarbonate transports (6). Alternatively, ADH could indirectly affect these latter transports by acting on the principal cells, which are involved in sodium absorption and potassium secretion, through changes in the transepithelial voltage (6). In fact, we also observed in the present study that dDAVP stimulated the fractional absorption of chloride in the distal tubule; other investigators also had previously found that ADH increases sodium absorption by the in vivo microperfused distal tubule of Sprague-Dawley rats (31), and dDAVP was found to increase sodium, chloride, and calcium absorption and potassium secretion in distal tubules of TPTX somatostatin-infused Brattleboro rats (29). Another important point deserves comment. Only one previous study by Capasso et al. (32) assessed the bicarbonate transport by means of the microcalorimetric method during free-flow conditions in the distal tubule of Wistar rats; in the control group of the latter study (32), net bicarbonate absorption was observed along the distal tubule, whereas net bicarbonate secretion was noted during the first period of hypotonic expansion in the present work. Considering the impressive effect of ADH on bicarbonate transport by the distal tubule in the present study and by the cortical collecting tubule in an in vitro study (6), the apparent discrepancy could be explained by differences in circulating ADH levels in rats of the previous (32) and those of the present study. Thus, we suggest that net bicarbonate secretion occurred in distal tubules of our rats because our experimental protocol restrained the endogenous ADH secretion.

Beside the distal tubule and cortical collecting tubule, ADH could also stimulate the proton secretion in the inner medullary collecting duct since this nephron segment possesses ADH receptors (9) and is a major site of urine acidification in the rat (22, 33). We have previously demonstrated that the principal cell that is the only cell type of the rabbit papillary collecting duct actively extrudes protons by a sodium gradient-independent electrogenic mechanism (34). Moreover, cyclic AMP and forskolin that activates adenylate cyclase have recently been shown to enhance bicarbonate absorption (proton secretion) in the medullary collecting duct from the inner stripe of outer medulla of rabbit kidney (35).

In addition to direct hormonal effects, stimulation of the renal proton secretion by an indirect consequence of the urine concentration may have contributed to the enhancement of urinary acidification during dDAVP infusion. In this connection, the process of the urine concentration could lead to luminal concentration of other factors that could secondarily stimulate the proton secretion by the tubular cells. In this regard, we have previously demonstrated that an increase in the urinary phosphate concentration is a potent stimulus to the collecting duct proton secretion (10, 11); the increase in the urinary phosphate concentration in the intact rats during dDAVP infusion in the present study may have contributed to

the stimulation of urinary acidification observed in these animals, but not to that in the TPTX somatostatin-infused rats in which there was virtually no phosphate in the urine. A possible role for other substances concentrated in the tubular fluid during dDAVP administration cannot be ruled out since it has been shown that undissociated weak acids, such as butyric and acetic acids, stimulate proton secretion in the turtle urinary bladder (36). Another indirect mechanism by which ADH administration could stimulate the proton secretion in collecting ducts is the following. Knepper et al. (37) demonstrated that enhancing the ambient total ammonia concentration stimulates proton secretion (or inhibits bicarbonate secretion, or both) in cortical collecting ducts. ADH could enhance NH_4^+ absorption in thick ascending limbs secondary to stimulation of sodium chloride absorption and subsequent increase in the lumen-positive transepithelial voltage (27); this would increase the total ammonia concentration not only in the adjacent interstitium surrounding cortical collecting ducts in the medullary rays, but also in that surrounding medullary collecting ducts by enhanced trapping of ammonia in the medulla secondary to counter-current multiplication. However, note that we evidenced stimulation of the loop chloride absorption during dDAVP infusion in TPTX somatostatin-infused, but not in intact rats in the present study; yet, stimulation of urinary acidification occurred in both groups of animals.

After the effects discussed above, net proton secretion was augmented in the distal parts of the nephron, the urine pH sharply decreased, and bicarbonate disappeared from the urine during the dDAVP infusion; the urinary excretion rate of titratable acid significantly increased secondary to the fall in urine pH. The urinary ammonium excretion rate did not increase despite the fall in urine pH, probably due to the decrease in the urinary flow rate since ammonia excretion is flow-dependent in relatively alkaline urine (38). Net acid excretion almost doubled in intact rats. Thus dDAVP administration increased the generation of new bicarbonate by the kidney. If of sufficient magnitude and/or duration, this could explain the maintenance of the plasma bicarbonate concentration within or slightly below the normal range despite water retention and urinary sodium loss in patients with the syndrome of inappropriate secretion of antidiuretic hormone (3) and normal dogs subjected to chronic ADH administration (2). Stimulation of urinary acidification restoring plasma bicarbonate concentration to normal during prolonged ADH administration in dogs with HCl-induced acidosis was ascribed to a measured increase in the aldosterone secretion probably due to severe hyponatremia (4). Obviously, such an explanation cannot account for the results obtained in the present acute experiments in which the aldosterone secretion was probably inhibited by volume expansion as attested by relatively high urinary sodium excretion rates and in which the extracellular fluid volume and plasma sodium concentration remained stable.

In conclusion, acute ADH administration is associated with marked stimulation of urinary acidification secondary to increased proton secretion or decreased bicarbonate secretion in the distal tubule and probably in the cortical collecting tubule. This could maintain the plasma bicarbonate concentration within the normal range despite water retention and secondary volume expansion during chronic antidiuretic states. ADH may be an important physiological determinant of urinary acidification.

Acknowledgments

We thank Chantal Nicolas for her secretarial assistance.

This study was supported by grants from the Institut National de la Santé et de la Recherche médicale (CRE 865003), the Centre National de la Recherche Scientifique (GRECO 24), the Université Paris 7, and the Fondation pour la Recherche Médicale Française.

References

1. Nutbourne, D. M., and H. E. de Wardener. 1960. The effect of a water diuresis on the urinary excretion of hydrogen ions in man. *Clin. Sci. (Lond.)* 20:63–73.
2. Lowance, D. C., H. B. Garfinkel, W. D. Mattern, and W. B. Schwartz. 1972. The effect of chronic hypotonic volume expansion on the renal regulation of acid–base equilibrium. *J. Clin. Invest.* 51:2928–2940.
3. Bartter, F. C., and W. B. Schwartz. 1967. The syndrome of inappropriate secretion of antidiuretic hormone. *Am. J. Med.* 42:790–806.
4. Cohen, J. J., H. N. Hulter, N. Smithline, J. C. Melby, and W. B. Schwartz. 1976. The critical role of the adrenal gland in the renal regulation of acid–base equilibrium during chronic hypotonic expansion. *J. Clin. Invest.* 58:1201–1208.
5. Nahum, H., M. Paillard, A. Prigent, F. Leviel, M. Bichara, J. P. Gardin, and J. M. Idatte. 1986. Pseudohypoaldosteronism type II: proximal renal tubular acidosis and dDAVP-sensitive renal hyperkalemia. *Am. J. Nephrol.* 6:253–262.
6. Tomita, K., J. J. Pisano, M. B. Burg, and M. A. Knepper. 1986. Effects of vasopressin and bradykinin on anion transport by the rat cortical collecting duct. *J. Clin. Invest.* 77:136–141.
7. Rouffignac, C. de, B. Corman, and N. Roinel. 1983. Stimulation by antidiuretic hormone of electrolyte tubular reabsorption in rat kidney. *Am. J. Physiol.* 244 (*Renal Fluid Electrolyte Physiol.* 13):F156–F164.
8. Kauker, M. L., J. T. Crofton, L. Share, and A. Nasjletti. 1984. Role of vasopressin in regulation of renal kinin excretion in long-Evans and diabetes insipidus rats. *J. Clin. Invest.* 73:824–831.
9. Morel, F. 1981. Sites of hormone action in the mammalian nephron. *Am. J. Physiol.* 240 (*Renal Fluid Electrolyte Physiol.* 9):F159–F164.
10. Bichara, M., O. Mercier, M. Paillard, and F. Leviel. 1986. Effects of parathyroid hormone on urinary acidification. *Am. J. Physiol.* 251 (*Renal Fluid Electrolyte Physiol.* 20):F444–F453.
11. Mercier, O., M. Bichara, M. Paillard, and A. Prigent. 1986. Effects of parathyroid hormone and urinary phosphate on collecting duct hydrogen secretion. *Am. J. Physiol.* 251 (*Renal Fluid Electrolyte Physiol.* 20):F802–F809.
12. Delahousse, M., O. Mercier, M. Bichara, and M. Paillard. 1987. Glucagon (GLU) inhibits urinary acidification. *Kidney Int.* 31:407. (Abstr.)
13. Woodhall, P. B., and C. C. Tisher. 1973. Response of the distal tubule and cortical collecting duct to vasopressin in the rat. *J. Clin. Invest.* 52:3095–3108.
14. Madsen, K. M., and C. C. Tisher. 1986. Structural-functional relationships along the distal nephron. *Am. J. Physiol.* 250 (*Renal Fluid Electrolyte Physiol.* 19):F1–F15.
15. Bichara, M., M. Paillard, B. Corman, C. de Rouffignac, and F. Leviel. 1984. Volume expansion modulates NaHCO_3 and NaCl transport in the proximal tubule and Henle's loop. *Am. J. Physiol.* 247 (*Renal Fluid Electrolyte Physiol.* 16):F140–F150.
16. Mercier, O., M. Bichara, M. Paillard, J. P. Gardin, and F. Leviel. 1985. Parathyroid hormone contributes to volume expansion-induced inhibition of proximal reabsorption. *Am. J. Physiol.* 248 (*Renal Fluid Electrolyte Physiol.* 17):F100–F103.
17. Mercier, O., A. Prigent, M. Bichara, M. Paillard, and F. Leviel.

1986. Effects of increase in plasma calcium concentration on renal handling of NaCl and NaHCO₃. *Am. J. Physiol.* 250 (*Renal Fluid Electrolyte Physiol.* 19):F441–F450.
18. Effendic, S., P. E. Lins, and R. Luft. 1978. Somatostatin and insulin secretion. *Metabolism.* 27:1275–1281.
19. Vurek, G. G., D. G. Warnock, and P. Corsey. 1975. Measurement of picomole amounts of carbon dioxide by calorimetry. *Anal. Chem.* 47:765–767.
20. Ramsay, J. A., R. H. J. Brown, and P. C. Croghan. 1955. Electrometric titration of chloride in small volumes. *J. Exp. Biol.* 32:822–829.
21. Sutton, R. A. L., and J. H. Dirks. 1981. Renal handling of calcium, phosphate, and magnesium. In *The Kidney*. 2nd ed. B. M. Brenner and F. C. Rector, Jr., editors. W. B. Saunders Co., Philadelphia. 551–618.
22. Graber, M. L., H. H. Bengel, E. Mroz, C. Lechene, and E. A. Alexander. 1981. Acute metabolic acidosis augments collecting duct acidification rate in the rat. *Am. J. Physiol.* 241 (*Renal Fluid Electrolyte Physiol.* 10):F669–F676.
23. Ichikawa, I., and B. M. Brenner. 1977. Evidence for glomerular actions of ADH and dibutyl cyclic AMP in the rat. *Am. J. Physiol.* 233 (*Renal Fluid Electrolyte Physiol.* 2):F102–F117.
24. Work, J., J. H. Galla, B. B. Booker, J. A. Schafer, and R. G. Luke. 1985. Effect of ADH on chloride reabsorption in the loop of Henle of the Brattleboro rat. *Am. J. Physiol.* 249 (*Renal Fluid Electrolyte Physiol.* 18):F698–F703.
25. Hall, D. A., and D. M. Varney. 1980. Effect of vasopressin on electrical potential difference and chloride transport in mouse medullary ascending limb of Henle's loop. *J. Clin. Invest.* 66:792–802.
26. Hebert, S. C., R. M. Culpepper, and T. E. Andreoli. 1981. NaCl transport in mouse medullary thick ascending limbs. I. Functional nephron heterogeneity and ADH-stimulated NaCl cotransport. *Am. J. Physiol.* 241 (*Renal Fluid Electrolyte Physiol.* 10):F412–F431.
27. Good, D. W., M. A. Knepper, and M. B. Burg. 1984. Ammonia and bicarbonate transport by thick ascending limb of rat kidney. *Am. J. Physiol.* 247 (*Renal Fluid Electrolyte Physiol.* 16):F35–F44.
28. Good, D. W. 1985. Sodium-dependent bicarbonate absorption by cortical thick ascending limb of rat kidney. *Am. J. Physiol.* 248 (*Renal Fluid Electrolyte Physiol.* 17):F821–F829.
29. Elalouf, J. M., N. Roinel, and C. de Rouffignac. 1984. Effects of antidiuretic hormone on electrolyte reabsorption and secretion in distal tubules of rat kidney. *Pfluegers Arch. Eur. J. Physiol.* 401:167–173.
30. DuBose, T. D., Jr., M. S. Lucci, R. J. Hogg, L. R. Pucacco, J. P. Kokko, and N. W. Carter. 1983. Comparison of acidification parameters in superficial and deep nephrons of the rat. *Am. J. Physiol.* 244 (*Renal Fluid Electrolyte Physiol.* 13):F497–F503.
31. Costanzo, L. S., and E. E. Windhager. 1980. Effects of PTH, ADH, and cyclic AMP on distal tubular Ca and Na reabsorption. *Am. J. Physiol.* 239 (*Renal Fluid Electrolyte Physiol.* 8):F478–F485.
32. Capasso, G., R. Kinne, G. Malnic, and G. Giebisch. 1986. Renal bicarbonate reabsorption in the rat. I. Effects of hypokalemia and carbonic anhydrase. *J. Clin. Invest.* 78:1558–1567.
33. Graber, M. L., H. H. Bengel, J. H. Schwartz, and E. A. Alexander. 1981. pH and PCO₂ profiles of the rat inner medullary collecting duct. *Am. J. Physiol.* 241 (*Renal Fluid Electrolyte Physiol.* 10):F659–F668.
34. Prigent, A., M. Bichara, and M. Paillard. 1985. Hydrogen transport in papillary collecting duct of rabbit kidney. *Am. J. Physiol.* 248 (*Cell Physiol.* 17):C241–C246.
35. Hays, S., J. P. Kokko, and H. R. Jacobson. 1986. Hormonal regulation of proton secretion in rabbit medullary collecting duct. *J. Clin. Invest.* 78:1279–1286.
36. Cannon, C., J. Van Adelsberg, S. Kelly, and Q. Al-Awqati. 1985. Carbon-dioxide-induced exocytic insertion of H⁺ pumps in turtle-bladder luminal membrane: role of cell pH and calcium. *Nature (Lond.)* 314:443–446.
37. Knepper, M. A., D. W. Good, and M. B. Burg. 1985. Ammonia and bicarbonate transport by rat cortical collecting ducts perfused in vitro. *Am. J. Physiol.* 249 (*Renal Fluid Electrolyte Physiol.* 18):F870–F877.
38. Orloff, J., and R. W. Berliner. 1956. The mechanism of the excretion of ammonia in the dog. *J. Clin. Invest.* 35:223–235.